UCRL--100212

DE91 006241

Zircaloy Cladding Degradation Under Repository Conditions

Lakshman Santanam
Graduate Research Assistant
Materials Engineering
Auburn University
Auburn, Alabama 36849

Suresh Raghavan
Graduate Research Assistant
Materials Engineering
Auburn University
Auburn, Alabama 36849

Henry Shaw
Technical Area Leader
Release Rates, NWMP
Lawrence Livermore National Laboratory
P.O. Box 808, L-204
Livermore, California 94550

Bryan A. Chin
Professor and Chairman
Materials Engineering
Ross Hall
Auburn University
Auburn, Alabama 36849

Abstract

Creep, a potential degradation mechanism of Zircaloy cladding after repository disposal of spent nuclear fuel, has been investigated. The deformation and fracture map methodology has been used to predict maximum allowable initial storage temperatures to achieve a thousand year life without rupture as a function of spent-fuel history. Maximum allowable temperatures are 340°C (613 K) for typically stressed rods (70-100 MPa) and 300°C (573 K) for highly stressed rods (140-160 MPa).

Key Terms: Zircaloy, repository, creep, stress corrosion, deformation and fracture maps

Introduction

The U.S. Department of Energy's Office of Civilian Radioactive Waste Management is investigating the suitability of the tuffaceous rocks at Yucca Mountain in Nevada for the permanent disposal of high-level radioactive waste and spent fuel. Regulatory requirements specify that in general the engineered barrier system must not release more than one part in 10^5 per year of the inventory of each radionuclide present at 1,000 years post-closure. This release requirement holds for 10,000 years post-closure.[1,2] The Zircaloy cladding that already exists on the fuel rod may be an important barrier that contributes to the ability to meet the above release requirement. This paper presents results from an investigation conducted in support of studies designed to address the integrity of the Zircaloy cladding after disposal in a tuff repository.

Three distinct time periods can be identified during repository storage:[3]

1. The high-temperature period during which the container is assumed to be unbreached, the fuel rods are surrounded by inert gas or air and no liquid water is present (0 to 90 years).

2. The intermediate-temperature period when the container is assumed to be unbreached and liquid water (from breached fuel rods containing water) may be present in contact with the fuel rods (90 to 1000 years).
3. The lower-temperature period when the container is assumed to be breached and air, water vapor and liquid water may be in contact with the spent fuel rods (1000 to 10,000 years and beyond). Water from well J-13 is currently thought to be similar to the water that may contact the breached canister.[4] The composition of J-13 well water may be found in reference 2.

Several potential mechanisms of Zircaloy cladding degradation during dry storage have been identified such as hydride reorientation, stress corrosion cracking, creep and creep fracture. A summary discussion of potential mechanisms of degradation is given by reference 2. This paper addresses only creep/creep fracture which is considered to be the dominant degradation mechanism during time period 1.

Creep and long-term fracture damage occurs during the inert gas isolation phase of the storage (period one). Deformation and fracture map analyses have been used to predict the time-to-rupture of Zircaloy-clad-spent Light Water Reactor (LWR) fuel subjected to various storage conditions. The questions that this analysis attempts to answer are how long and under what temperature conditions the fuel can be reasonably claimed to be unfailed. In the repository, temperatures are anticipated to rise first as the repository is filled and then decrease with increasing time due to a decay in the heat generation rate of the spent fuel. In this analysis, a life fraction rule has been used to account for changing temperature and stress conditions. This life fraction rule has been combined with the results of deformation and fracture maps to predict maximum allowable temperatures to achieve a 1000 year life.

Deformation and Fracture Maps

Background

One of the probable mechanisms of failure during the inert gas isolation phase is creep rupture failure. Previous predictions of Zircaloy cladding failure have been based on direct extrapolation of existing short term data [5,6] or have assumed a single equation, like the Larson-Miller parameter [7], to describe the failure mechanisms. These methods ignore changes in the deformation and failure mechanisms as the stress and temperature conditions are altered and resulting failure times change. Such analyses are very useful for interpolation between existing data fields but often lead to erroneous results when extrapolated to regimes involving different deformation and failure phenomena.[8]

Deformation and fracture maps enable predictions of the dominant deformation and failure mode for varying temperature and stress regimes, as well as varying irradiation histories.[8] Deformation and fracture maps can be generated using the model based method in which different theoretical expressions for deformation or fracture are evaluated. The mechanism with the highest deformation rate is assumed to be the dominant mechanism. Similarly,

in the generation of the model-based fracture map, values of time-to-failure are numerically evaluated for possible fracture mechanisms, with the assumption that the mechanism with the shortest failure time controls the fracture. An empirical life fraction rule is combined with the results of the deformation and fracture maps to predict acceptable storage and disposal temperatures.

Analysis Method

The deformation and fracture map methodology has been applied in the licensing of several dry storage facilities. A detailed description of the methodology can be found in references 7,8. The present work describes modifications to dry storage deformation and fracture maps to predict cladding response for assumed repository conditions over a 1000-year period. This included the selection of a function to model the temperature decay history of the repository, refinement of the parameters that control the recovery process to better describe the region of lower repository temperatures, and incorporation of variable time steps to improve the accuracy of cumulative damage predictions at early times where the temperature is changing rapidly.

Selection of temperature decay function. The projected peak cladding temperature as a function of time in a tuff repository is shown in Figure 1[2]. This temperature history is based upon horizontal emplacement in a repository at 44 kW/acre of a canister containing 10 year old spent fuel (3.3 kW) with 12 internal fins. This temperature curve can be approximated by the equation given below, which was then incorporated into the models:

$$T\ (K) = T_o\ (K) * (\text{time in months})^{-0.1041} \qquad (1)$$

Selection of melting temperature. The experimental melting temperature of beta phase Zircaloy, used in the dry storage predictions, was replaced by the theoretical melting temperature of alpha phase Zircaloy (calculated to be 1900 K). Based upon a review of the pertinent literature [9] regarding the use of the theoretical melting temperature of alpha zirconium, it was concluded that a better description of the annealing and dislocation motion process (which occur in the alpha Zircaloy phase), could be obtained by using the theoretical alpha Zircaloy melting temperature instead of the beta Zircaloy melting temperature. All applications of the deformation and fracture map models to the repository case involve only the alpha phase. Use of the beta Zircaloy melting temperature results in a prediction that underestimates the recovery process.[9]

Incorporation of variable time steps. Another modification involved incorporation of variable time steps to calculate the cumulative damage. Small time steps correspond to small temperature and stress changes, which improve the accuracy of cumulative damage calculations. The variable time step employed utilizes small time steps when the temperature is changing rapidly and larger steps as the rate of temperature change decreases.

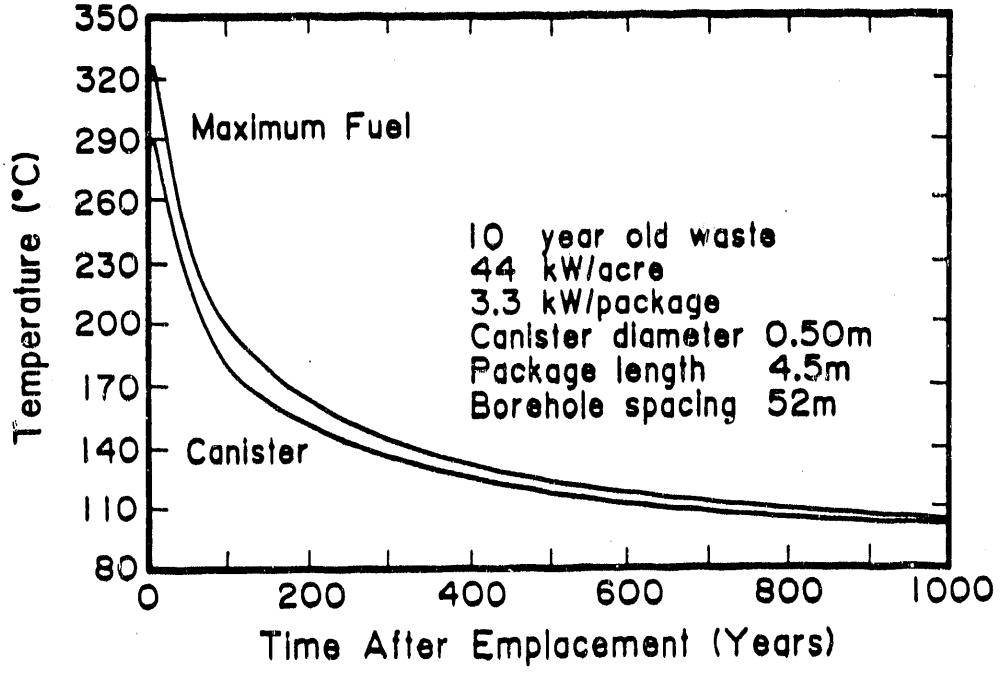

Figure 1. Peak Fuel and Canister Temperature as a Function of Time (After Rothman reference 2)

Calculations

Table 1 lists the deformation equations used in the analyses and Table 2 lists the coefficients and the symbols used in the equations. Table 3 lists the reduced deformation equations after substitution of these coefficients. Table 4 lists the fracture equations; Table 5 shows the symbols and coefficients used in these equations and Table 6 lists the reduced fracture equations.

Deformation rates were evaluated from the equations listed in Table 3. The dominant deformation mechanism is the one with the highest deformation rate. Values of time-to-failure were determined from the equations in Table 6. The mechanism with the least time to failure controls the fracture. Note that the equations in Table 6 are dependent upon the deformation rate which is calculated from the Equations of Table 3. A detailed description of the development of the equations and their use is given in references 8,10.

A life fraction rule was used to account for changing temperature and stress conditions. Temperatures are assumed to decrease with increasing time as per equation (1) after the initial warm up period. Additionally the stress in the cladding will decrease due to cladding creep and a decrease in the fission gas pressure due to decreasing temperature. Small increases due to helium gas production from actinide decay were neglected for this 1000-year analysis. This life fraction rule can be mathematically represented as follows:[8]

$$1 = \frac{\Delta t_1}{\tau_1} + \frac{\Delta t_2}{\tau_2} + \frac{\Delta t_3}{\tau_3} + \ldots, \qquad (2)$$

or

$$\sum_{i=1}^{N} \frac{\Delta t_i}{\tau_i} = 1 \qquad (3)$$

where Δt_i is the time spent at the i^{th} temperature, and τ_i is the time required to fracture a specimen under isothermal, isostress testing conditions. When the cumulative damage fraction ($\Delta t_i/\tau_i$) reaches one, the fuel rod is assumed to have failed.

Results

It is assumed that the fuel rods will have a temperature decay history as described by equation 1. To determine the maximum allowable temperatures, a computer program was developed. This program uses the deformation and fracture map methodology in conjunction with the life fraction rule to predict behavior in the repository. The results are depicted in Figure 2, which is a plot of maximum allowable peak temperature as a function of clad hoop stress for 10 year old spent fuel (10-years in wet storage) and an initial clad stress of 70 MPa. This maximum allowable temperature is the maximum peak temperature (for a given initial clad stress) following the temperature decay rate shown in Figure 1 that yields a cumulative damage fraction of less than one after an elapsed time of 1000 years.

Table 1

Deformation Equations

High Temperature Climb	$\dot{\epsilon}_{HT} = A_1 \cdot D_{ol} \cdot \exp(-Q_1/RT) \cdot \frac{Eb}{KT} \cdot (\sigma/E)^n$
Low Temperature Climb	$\dot{\epsilon}_{LT} = 50 \cdot A_1 \cdot D_{oc} \cdot \exp(-Qc/RT) \cdot \frac{Eb}{KT} \cdot (\sigma/E)^{n+2}$
Grain Boundary Sliding	$\dot{\epsilon}_{GBS} = A_{GBS} \cdot D_{ogb} \cdot \exp(-Qgb/RT) \cdot \frac{Eb}{KT} \cdot (b/d)^3 \cdot (\sigma/E)^2$
Nabarro-Herring	$\dot{\epsilon}_{NH} = A_{NH} \cdot D_{ol} \cdot \exp(-Q_1/RT) \cdot \frac{Eb}{KT} \cdot (b/d)^2 \cdot (\sigma/E)$
Coble	$\dot{\epsilon}_{CO} = A_{CO} \cdot D_{ogb} \cdot \exp(-Qgb/RT) \cdot \frac{Eb}{KT} \cdot (b/d)^3 \cdot (\sigma/E)$

Table 2

Symbols and Coefficient Values for Deformation Equations

$\dot{\epsilon}$ - strain rate

σ - stress

T - temperature

R - gas constant = 8.3144 J/mole-K

k - Boltzmann's constant = 1.38×10^{-29} MJ/K

b - Burger's vector = 3.23×10^{-10} m

d - grain size = 5.0×10^{-6} m

T_m - melting temperature of Zircaloy = 2125K

E - Young's Modulus $(11.81 - 14.59\ T/T_m) \times 10^4$ MPa, $T_m/T > 4.06$
for $T < 865°C$ $(11.09 - 11.61\ T/T_m) \times 10^4$ MPa, $T_m/T < 4.06$

n - stress exponent = 5

Q - activation energy

Q_l - 250 kJ/mol

Q_{gb} - 175 kJ/mol

Q_c - 180 kJ/mol

D_o - diffusivity coefficient

D_{ol} - 2.00×10^{-4} m^2/s

D_{ogb} - 3.89×10^{-6} m^2/s

D_{oc} - 2.26×10^{-6} m^2/s

A - strain rate coefficient

A_l - 7.4×10^{-7}

A_{CO} - 5.362×10^2

A_{GBS} - 8.85×10^6

A_{NH} - 0.92

A_{GBL} - 5×10^2

Table 3

Reduced Deformation Equations

High Temperature Climb	$\ln\dot{\epsilon}_{HT} = 5\cdot\ln(\sigma/E)+55.75-14.15(T_m/T)+\ln(T_m/T)+\ln(E/10^4)$
Low Temperature Climb	$\ln\dot{\epsilon}_{LT} = 7\cdot\ln(\sigma/E)+55.18-10.19(T_m/T)+\ln(T_m/T)+\ln(E/10^4)$
Grain Boundary Sliding	$\ln\dot{\epsilon}_{GBS} = 2.\ln(\sigma/E)+20.74-9.9036(T_m/T)+\ln(T_m/T)+\ln(E/10^4)$
Nabarro-Herring	$\ln\dot{\epsilon}_{NH} = \ln(\sigma/E)+18.25-14.15(T_m/T)+\ln(T_m/T)+\ln(E/10^4)$
Coble	$\ln\dot{\epsilon}_{CO} = \ln(\sigma/E)+11.03-9.9036(T_m/T)+\ln(T_m/T)+\ln(E/10^4)$

Table 4

Fracture Equations

Theoretical Shear Strength	$\sigma_{th} = \left(\frac{E\gamma_f}{a_o}\right)^{1/2} \approx \frac{E}{10}$
Transgranular Fracture	$t_f^{TG} = \epsilon_n + \left(\frac{1}{4.937}\right)\left(\frac{n}{n-1}\right)\ln\frac{0.38}{f_v^{1/2}} - 1\ \dot{\epsilon}^{-1}$
Triple-Point Cracking	$t_f^{TP} = \frac{f}{Ed}\left(\frac{\sigma}{E}\right)^{-1}\dot{\epsilon}^{-1}$
Cavitation-Diffusional Growth	$t_f^{CD} = \frac{2.525 \times 10^{-3}\ \ell^3}{\delta D_{ogb} b^2 \exp\frac{-Q_{gb}}{RT}}\left(\frac{kT}{Eb}\right)\left(\frac{\sigma}{E}\right)^{-1}$
Cavitation--Power Law Growth	$t_f^{CP} = \frac{(1 - 0.78\ P_o\ \ell_o)}{4.87}\dot{\epsilon}^{-1}$

Table 5

Symbols and Coefficient Values for Fracture Equations

t_f - time to fracture

ϵ_n - hole nucleation strain - 0.08

f_v - volume fraction of intragranular inclusions - 0.025

P_o - average particle diameter - 100 Å

ℓ_o - particle spacing along boundary - 2.0×10^{-6} m

ζ - $\dot{\epsilon}_{GBS}/\dot{\epsilon}$ - contribution of grain boundary strain rate to total strain rate - 0.2

ℓ - average cavity spacing - 2.6×10^{-6} m (6 per grain segment)

δ - width of grain boundary - 1.6×10^{-8} m (50 Burger's vectors)

γ_f - free surface energy created by fracture - 35 J/m^2

a_o - lattice spacing

Table 6

Reduced Fracture Equations

Transgranular Fracture	$\ln t_f^{TG} = -1.797 - \ln \dot{\epsilon}$
Triple-Point Cracking	$\ln t_f^{TP} = -5.655 - \ln \dot{\epsilon} - \ln \frac{\sigma}{E} - \ln \frac{E}{10^4}$
Cavitation--Diffusional Growth	$\ln t_f^{CD} = +4.15 - \ln \dot{\epsilon}_{gbs} + \ln \frac{\sigma}{E}$
Cavitation--Power Law Growth	$\ln t_f^{CP} = -1.587 - \ln \dot{\epsilon}$

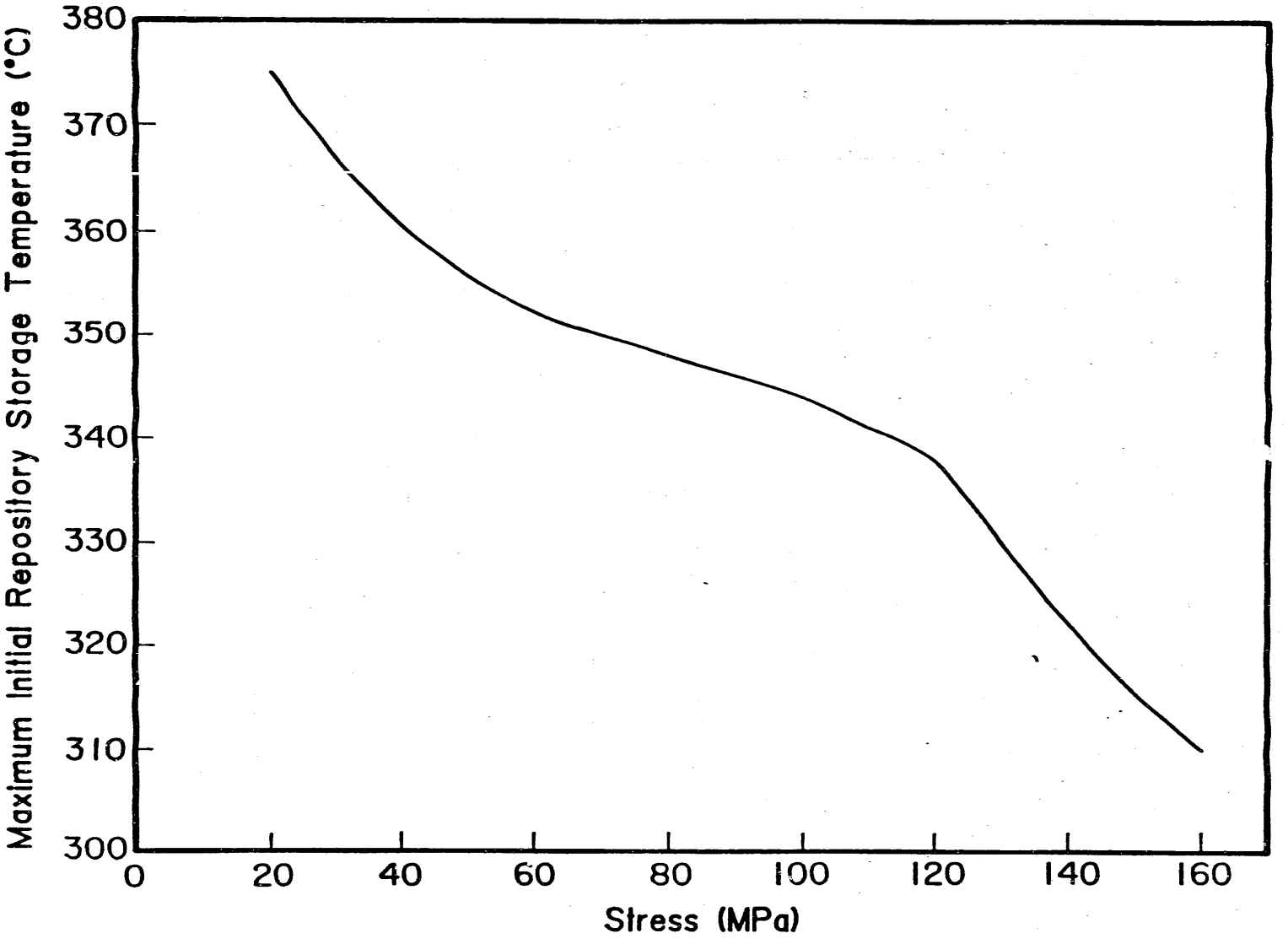

Figure 2. Predicted Peak Repository Temperature as a Function of Initial Fuel Rod Stress

For times of 1000 years and beyond the damage accumulation rates are so low (because of the low repository temperatures) that calculations beyond 1000 years are not necessary.

For typically stressed rods (70 -100 MPa) with low fission gas release, initial temperatures of 340°C would be acceptable. However for high burnup rods with large fission gas release that results in highly stressed rods (140-160 MPa), initial temperatures should not exceed 300°C. It should be noted that the predicted maximum allowable temperature is a function of initial clad stress (fuel rod history), age of spent fuel (cumulative time spent in wet storage) and anticipated temperature history of the repository. The calculations are conservative for spent fuel that is younger than 10 years post discharge, but nonconservative for older fuel rods. This dependence upon time since discharge results from the higher rates of temperature decay in younger spent fuel versus older spent fuel. Additionally, the temperature history curve shown in Figure 1 does not include the initial region of temperature increase that occurs during filling of the repository.

Conclusions

Zircaloy cladding is potentially an effective barrier to the release of radionuclides from spent fuel in a repository. After making some assumptions about Zircaloy material behavior, preliminary models have been developed to address maximum storage temperature limits. The following conclusions resulted from this preliminary study:

Based on a deformation and fracture map analysis, predictions of maximum allowable temperatures for cladding stresses from 20 MPa to 160 MPa have been made for times upto 1000 years post-emplacement. Maximum allowable temperatures are 340°C (613 K) for typically stressed rods (70 -100 MPa) and 300°C (573 K) for highly stressed rods (140 -160 MPa).

Sponsorship

This work was performed for the Yucca Mountain Project (YMP) under the direction of the University of California, Lawrence Livermore National Laboratory as part of the U.S. Department of Energy Office of Civilian Radioactive Waste Management Program. The Yucca Mountain Project work is managed by the Yucca Mountain Project Office (YMPO) of the U.S. Department of Energy, Nevada Operations Office (DOE/NV).

Acknowledgements

The authors are indebted to Dr. Ray Stout, Lawrence Livermore National Laboratory, California, Dr. Nels Madsen of Auburn University, for the many useful discussions.

References

1. U. S. Office of the Federal Register Code of Federal Regulations, Title 10, Energy, Part 60, Subpart D, Section 60.113, "Disposal of High-Level Radioactive Wastes in Geologic Repositories: Licensing Procedures."

2. A. J. Rothman, "Potential Corrosion and Degradation Mechanisms of Zircaloy Cladding on Spent Nuclear Fuel in a Tuff Repository," UCID-20172, September 1984.

3. H. D. Smith, "Zircaloy Cladding Corrosion Degradation in a Tuff Repository," HEDL-7455, Rev. 1, July 1985, p. 12.

4. H. D. Smith, "Initial report on Stress Corrosion Cracking Experiments Using Zircaloy-4 Spent Fuel Cladding Rings," Westinghouse Hanford Company, Richland, WA.

5. L. D. Blackburn et. al., "Maximum Allowable Temperature for Storage of Spent Nuclear Fuel - An Interim Report," HEDL-TME 78-37, UC-70, 1978.

6. E. R. Einziger, D. M. Bozi, and A. K. Miller, "Transactions," Waste Form Development and Processing, American Nuclear Society, 1980, p.131.

7. A. K. Miller, "Application of the SCCIG Model to Dry Storage of Spent Fuel," Workshop on Spent Fuel Integrity in Dry Storage, Seattle, WA, Jan. 20, 1982.

8. M. A. Khan, N. H. Madsen, and B. A. Chin, "Fracture Predictions in Zircaloy Fuel Cladding," Effects of Radiation on Materials: Twelfth International Symposium, ASTM Stp 870, Philadelphia, 1985, pp. 642-655.

9. A. J. Ardell, "On the Calculation of Melting Temperatures for Low-Temperature phases of Polymorphic Metals," Acta Metallurgica, Vol. 11, June 1963, pp. 591-594.

10. B. A. Chin and E. R. Gilbert, "Prediction of Maximum Allowable Temperatures for Dry Storage of Zircaloy-Clad Spent Fuel in Inert Atmosphere," Nuclear Technology, V85, April 1989, pp. 57-65.

Appendix A

This report does not use any information from the Reference Information Base nor contain any candidate information for the Reference Information Base or the Site and Engineering Properties Data Base (SEPDB).

-END-

DATE FILMED

01 / 29 / 91